



Contents lists available at ScienceDirect

Surface Science

journal homepage: www.elsevier.com/locate/susc

Growth morphology of ultra-thin Ni films on Pd(100)

C. Parra*, P. Häberle

Departamento de Física, Universidad Técnica Federico Santa María, 2390123 Valparaíso, Chile

ARTICLE INFO

Article history:

Received 8 April 2009

Accepted for publication 8 October 2009

Available online xxxxx

Keywords:

Metallic heteroepitaxy

Ultra-thin Ni films

Strain

Scanning tunneling microscopy

ABSTRACT

A series of thin Ni films, with thicknesses between 0.2 ML to 13 ML, were deposited on a Pd(100) substrate ($a = 3.89 \text{ \AA}$) at room temperature (RT). The growth morphology was investigated using scanning tunneling microscopy (STM). STM images indicate the existence of three different growth modes as a function of increasing coverage. Up to 6.5 ML, the films grow pseudomorphically, consistent with a face-centered tetragonal (fct) structure. From 6.5 ML to 10.5 ML a new apparent interlayer distance of $1.0 \pm 0.1 \text{ \AA}$ is established. The new structure is accompanied by the appearance of an arrangement of filaments on the top layer surface. These filaments are presumably related to a strain relief mechanism of the fct films. Finally above 10.5 ML the Ni films recover the face-centered cubic (fcc) lattice constants. The filaments evolve, as a function of coverage, to form a net-like structure over the whole surface.

© 2009 Elsevier B.V. All rights reserved.

1. Introduction

By depositing ultra-thin metallic films of a certain element on top of a single crystal surface of a different material, it is possible to stabilize the adsorbate atomic positions in structures which deviates substantially from those shown by the bulk of the same element. By choosing the proper heteroepitaxial system and controlling features such as roughness, strain induced by lattice mismatch and atomic intermixing between film and substrate, not only the structural parameters can be modified but also some intrinsic physical properties of the adsorbed element. These metastable artificial structures recover finally their bulk parameters when the film exceeds a certain critical thickness, usually a few monolayers in most cases. These structural transformations are observed to be rather sharp and occur through an abrupt distortion, which is accompanied by a strong morphological reorganization. As expected these systems also exhibit changes in other physical properties, for example the film magnetization [1]. A well-documented case of one of such systems is Fe/Cu(100) [2–6]. Inspired by the correlation between structure and magnetism in this particular case [7–10], we have investigated the structure of Ni films grown on Pd(100). Since both Ni and Pd have different lattice parameters, the morphology of the Ni films, in case of epitaxial growth, should be dominated by lattice strain effects. We have characterized the growth of these films with STM. The Pd fcc substrate has been chosen in order to favor a contraction of the Ni film in the vertical direction (tetragonal distortion-fct) due to an increased tensile intralayer strain. This distortion, due

to the resulting pseudomorphic growth and the lattice misfit, is characterized by a large tensile strain, $m = 10.5\%$, in the Ni overlayer. While there are few previous reports [11–13] which have focused on the structure of the strained Ni films, there is almost no information regarding the evolution of the structural morphology in this system. For RT growth, the existing diffraction studies [11–13] show the formation of a tetragonally distorted structure, induced by the Ni epitaxial growth. For thicknesses beyond 12 ML, the structure turns into a bulk-like Ni fcc structure. In the following section we present some experimental details regarding the sample preparation and measurements conditions. In Section 3, the STM measurements are presented together with the analysis of the surface structure evolution, based on the topographic images. Finally, in the analysis section, we summarize and discuss these results.

2. Experimental details

Ni overlayers (0.2–13 ML) were grown on a (100)-oriented Pd single crystal at RT. As the Ni source a high-purity rod was used, heated by electron bombardment in ultra-high vacuum conditions (UHV). The typical evaporation pressure was below 7×10^{-10} torr. Background oxygen contamination of the as-deposited Ni films was estimated, by Auger electron spectroscopy (AES), to be less than 1.5%.

Prior to deposition, the substrate surface was prepared by a series of RT Ar^+ sputtering cycles at 1 keV, followed by a 20 min anneal up at 910 K. This procedure was repeated until a clean and well-ordered surface with large atomically flat terraces was obtained as confirmed by AES and Low energy electron diffraction (LEED). The LEED screen displays a sharp $p(1 \times 1)$ pattern for a

* Corresponding author. Tel.: +56 32 2654724; fax: +56 32 2797656.
E-mail address: carolina.parra@usm.cl (C. Parra).

60 eV primary electron beam energy. An initial S contamination was eliminated by argon-ion bombardment of the surface at 550 °C for about 2 h. The Ni vapor beam impinges the room-temperature Pd substrate at an angle of 15° from the normal direction. The Ni deposition rate on the sample was estimated to be 0.6 Å/min. This value was crossed checked with a quartz microbalance (QMB) and other experimental techniques available in the system (STM, Reflection high energy electron diffraction (RHEED) and AES). Due to the careful calibration of the films thicknesses, the actual coverage was determined to be within 0.1 ML, of the value indicated by the QMB corrected by the appropriate tooling factors. All the STM images were taken in constant-current mode (0.1–0.2 nA) with a negative sample bias voltage, typically 900 mV.

3. Results and discussion

The overview image of the clean Pd substrate (Fig. 1) shows the presence of flat terraces, around 100 nm wide, and monoatomic steps. The line profile indicates a corrugation consistent with monoatomic steps.

Figs. 2–4, show the evolution of the Ni/Pd(100) surface, as a function of Ni overlayer coverage. For low coverages, 0.2 ML (Fig. 2a) the Pd surface is covered randomly by one monolayer height Ni islands, with an average size around 2.6 nm². The islands show no preferential nucleation sites and have random shapes, whose internal atomic structure could not be resolved by the STM. The islands density at this early stage is 4.3×10^{-2} islands/nm². Fig. 2b display the surface for 0.9 ML. The first layer islands are close to the percolation limit [14]. Many of the islands are now interconnected across the terraces, forming an irregular network with a few unconnected smaller islands. At this coverage some second layer islands are detected, hence this coverage is the onset for second layer growth. This late second layer growth is indeed relevant for the resulting film structure [15–18]. Smooth films, growing layer-by-layer, can only be established if stable second layer clusters form after the coalescence of islands in the first layer. While second layer nucleation, preceding island coalescence, leads to a rough film morphology.

Fig. 2c shows the surface morphology for 2.0 ML. The second layer islands are partially interconnected at this coverage and they have a more rectangular shape (see inset) with edges oriented preferentially along [011] and $\bar{0}\bar{1}\bar{1}$ crystallographic directions. At 4.0 ML (Fig. 3a), the almost rectangular shape of the structures seen at 2.0 ML is better defined by the additional material.

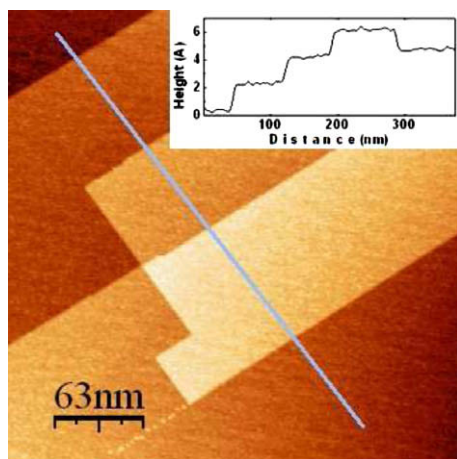


Fig. 1. STM image of the Pd(100) substrate. Scanning area: 313 × 313 nm². The line profile shows single atomic steps in agreement with the expected height difference between Pd atomic layers.

Through careful comparison of STM images from successive deposits, we can follow the evolution of the different layers exposed at the surface. The estimation of the depth of the overlayers, in a particular section of the surface, is based on the assumption that the extent of a particular layer, a fixed height in a STM topographic image, increases monotonically with coverage.

For example at 5.5 ML Ni, the sixth layer islands have an average width of 11.90 ± 0.31 Å and a monoatomic step height of 1.55 ± 0.13 Å. This interlayer spacing is different from that displayed by bulk Ni along the [001] direction. Nevertheless it agrees well with the expected lattice spacing for fct growth [19].

Fig. 3b shows the surface after deposition of $\theta = 6.5$ ML. From this image we can obtain 2.6% of a Ni ML is required to complete the fifth layer, likewise 7.3% of the sixth layer atoms are absent, meaning this layer filling factor is 92.7%. The corresponding filling factors for the seventh and eighth layers are 29% and 1.5%. Hence, for this particular coverage, the surface exhibits a height fluctuation limited to four atomic layers. In addition, the height distribution for this coverage displays a singular behavior: the depths of the holes in the sixth layer are on average 1.56 ± 0.12 Å, in agreement with the values shown in previous coverages, while the height of the seventh layer islands is only 1.00 ± 0.11 Å. The surface morphology, as in the previous case, is dominated by the seventh layer islands aligned along crystallographic directions (see insert in Fig. 3b). The average width of these structures is 12.96 ± 3.18 Å. A similar behavior is obtained for 7.5 ML in which the top layer exhibits wavy filament-like structures (Fig. 3c), with an apparent height of 0.98 ± 0.17 Å and an average width of 5.25 ± 3.65 Å. The new interlayer distance is not related to any known crystallographic Ni spacing, so no simple atomic model can be provided to describe the film structure. A similar value for the height of the elongated islands is observed also for higher coverages, up to 10.5 ML (see Fig. 5).

Beyond 10.5 ML a new interlayer distance of 1.76 ± 0.10 Å is established, for islands in the eleventh layer (see Fig. 6). This value is indeed consistent with the reestablishment of the Ni fcc structure. At this coverage, the surface displays a rectangular network formed by straight filaments (Fig. 4a). For 11.9 ML (Fig. 4b), these filaments start to cross each other leading to the formation, at higher coverages, of a rectangular net-like structure (see 12.5 ML, Fig. 4c) which interconnects the whole surface as a weft. The height of the connecting threads is 1.74 ± 0.2 Å with a characteristic spacing between them of 50.15 ± 3.6 Å.

Fig. 6 summarizes the evolution of the interlayer distances as a function of Ni coverage. The characteristic value for this parameter, obtained from similar quality STM images, remains constant for bias voltages between 0.5 eV and 1.4 eV. Three regions can be distinguished; up to 6.5 ML, the Ni films show a mean height of 1.53 Å in agreement with the fct epitaxial growth prediction of 1.52 Å [20]. For higher coverages, the interlayer distance diminishes abruptly to a value close to 1 Å which is maintained over the following four layers. The interlayer spacing of the eleventh layer is changed again, this time to a larger value, in agreement with the corresponding bulk value for fcc Ni (1.76 Å).

Fig. 7 shows the layer distribution versus coverage for the Ni/Pd(100) system. The y-axis indicates the fraction of the surface which can be attributed to a particular layer and the x-axis is the coverage as indicated by the QMB. It shows for example that only around 0.9 ML the second layer starts to grow. For a total mass of 1 ML of Ni, 93% of the first layer is completed while the remaining fraction of the surface appears as second layer islands. From 2 ML and up multilayer growth is the dominant process. Between 2.0 and 6.5 ML, the films display three-layers simultaneously while above 6.5 ML a total of four different levels can be resolved in the topographic images (see insert in Fig. 7).

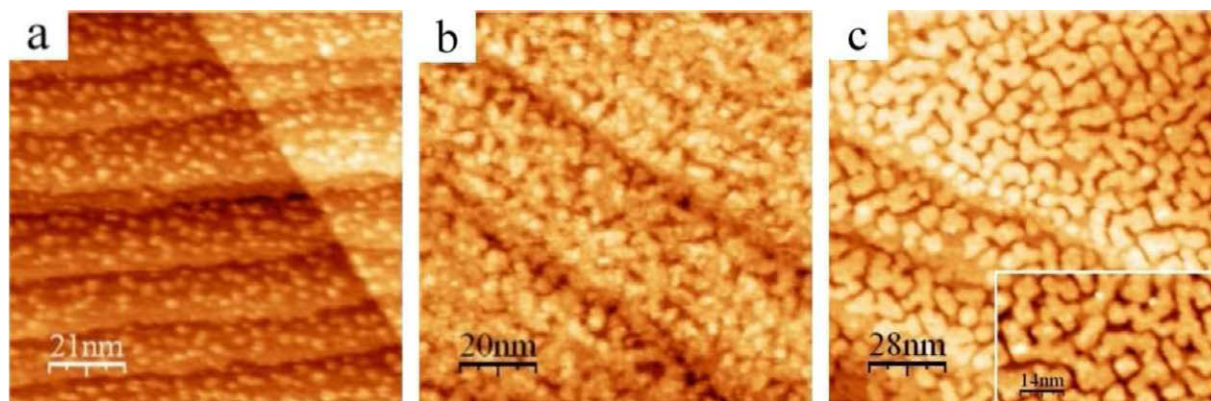


Fig. 2. STM images of Ni on Pd(100), from early growth up to the completion of the second monolayer. The characteristic deposition rate was 0.30 ML/min. (a) $\Theta = 0.2$ ML, (b) $\Theta = 0.9$ ML and (c) $\Theta = 2.0$ ML. The Ni atoms form 2D clusters. The percolation limit is reached around 0.9 ML, just when the second layer starts to grow. A layer-by-layer growth mode is maintained up to 2.0 ML. From here on the growth involves multiple layers.

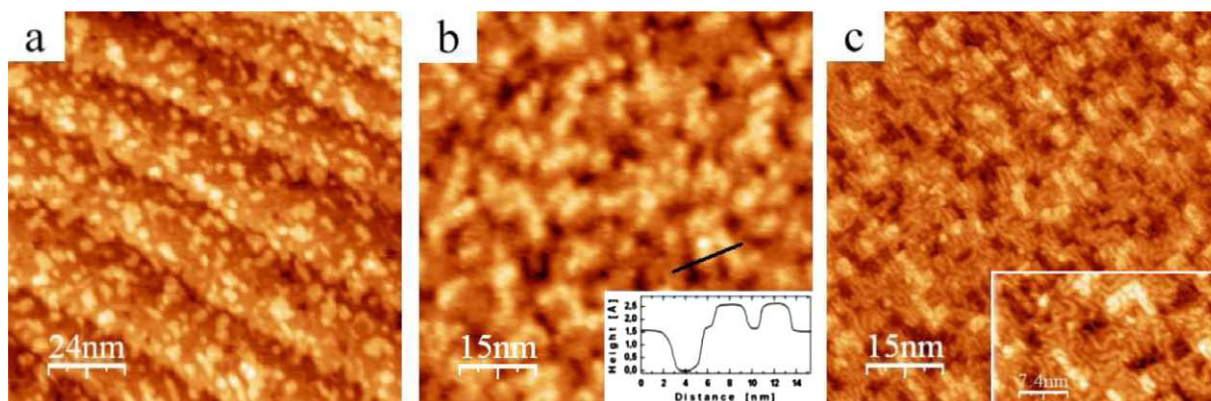


Fig. 3. Ni films, RT-deposited on Pd(100): (a) $\Theta = 4.0$ ML, (b) $\Theta = 6.5$ ML, and (c) $\Theta = 7.5$ ML. The inset in Fig. 4b shows a line scan in which two interlayer distances can be identified. A singularity in the interlayer height appears at 6.5 ML. The new apparent height is close to 1 Å. The internal structure of the new terraces is formed by wavy like-filaments which are clearly distinguished in Fig 3c.

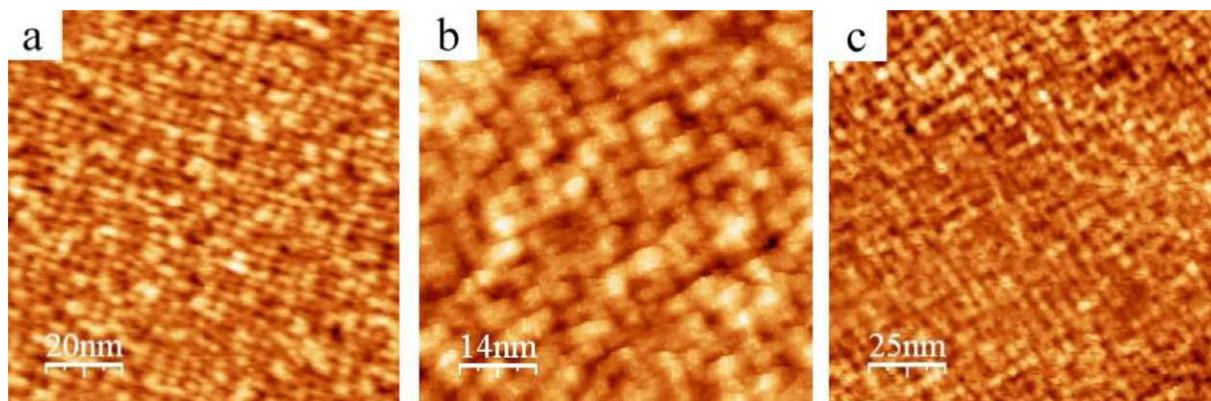


Fig. 4. STM topographic images: (a) $\Theta = 10.5$ ML, (b) $\Theta = 11.9$ ML, (c) $\Theta = 12.5$ ML. For 10.5 ML, the film recovers the Ni bulk inter layer parameters. The surface morphology evolves from rectangular islands for 10.5 ML to a net-like structure connecting the whole surface for a thickness 12.5 ML.

Fig. 8 displays the surface roughness obtained from the STM images [21]. According to its characteristic features, the three growth regions can also be identified in this graph. As shown in the plot, up to 2 ML, the surface roughness oscillates around the average height with an approximate periodicity of 1 ML. The minimum roughness values (points A and B) for each oscillation correspond to an integral number of layers. This particular behavior is in agreement with the evolution of the surface roughness for the case

of a film grown in a near layer-by-layer mode. As we have already shown in Fig. 7, multilayer growth starts at 2 ML. Up to 6.5 ML (region II) three levels for each particular coverage are observed, which agrees with the larger average roughness displayed in this region. A similar behavior has been observed in previous measurements of the RHEED intensity in the same system [19]. The associated changes in roughness are related to the transition from a layer-by-layer mode to a multilayer growth mode. As expected

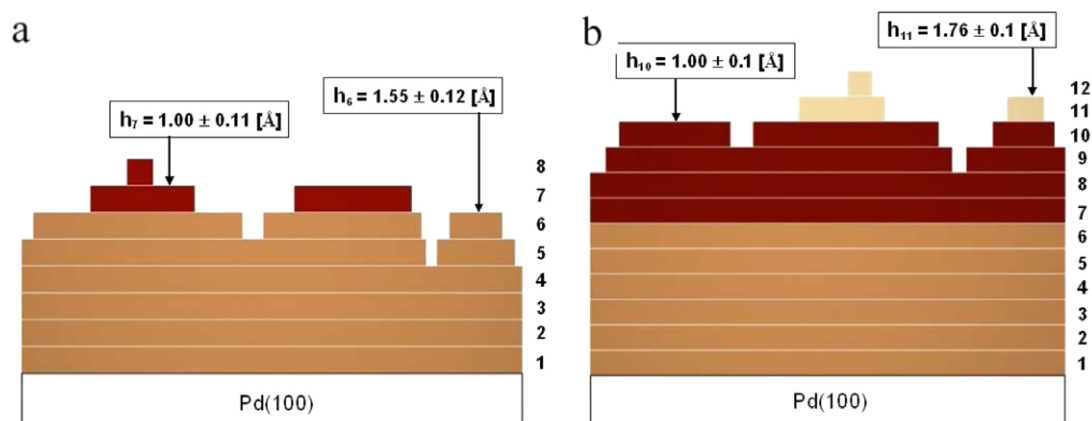


Fig. 5. Schematic cross section of the film for: (a) 6.5 ML of Ni/Pd(100). The seventh layer islands height displays a value around 1 Å in contrast with the average fct value of 1.55 Å shown by the sixth layer. (b) 10.5 ML. The same interlayer distance is maintained, for coverages between 7 and 10 ML. This particular section of the film, with the new interlayer distance, has been highlighted with a darker color in the figure. Beyond 10 ML Bulk Ni parameters are recovered. (For interpretation of the references to colour in this figure legend, the reader is referred to the web version of this article.)

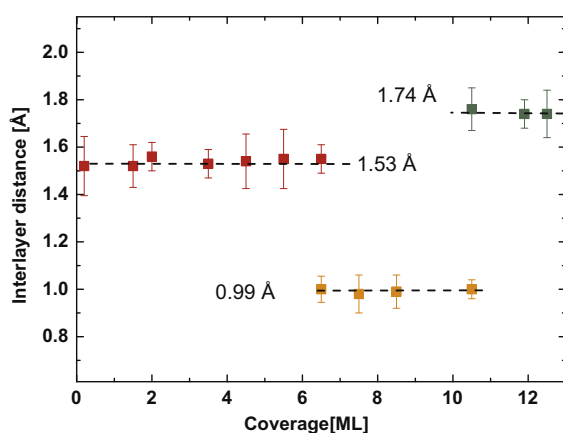


Fig. 6. Ni interlayer distance as a function of coverage. Three characteristic growth regions can be identified: up to 6.5 ML the film grows pseudomorphically over the Pd substrate, with a fct structure. A transition region occurs between 6.5 and 10.5 ML, where the films show a new interlayer distance close to 1 Å. Above this coverage the films recover their bulk parameters.

the average roughness increases again above 6.5 ML, since for these coverages, four different layers are exposed on the surface

4. Analysis

In summary, the STM topographic images demonstrate the existence of three growth regions for Ni on Pd(100). Up to 6.5 ML the films grow pseudomorphically, displaying a fct structure with a mean interlayer distance of 1.53 Å, in agreement with linear elasticity theory [20]. In the sub-monolayer regime, the surface morphology is characterized by a distribution of randomly shaped 2D Ni clusters on the Pd substrate.

The fact that the islands have irregular shape at the initial stage of growth can be explained by the large tensile strain on the top layer. Due to strain there is a substantial reduction of the edge and kink diffusion energy barriers, thus promoting atomic detachment from the islands perimeter. This process favors a random orientation for the islands lateral growth [22–26]. Up to 2 ML the films grow in a nearly perfect layer-by-layer mode. Above 2 ML the surface exposes three layers, indicating the beginning of multilayer growth. Simultaneously with this change, the islands assume a well-defined-rectangular shape. This type of symmetry is also ob-

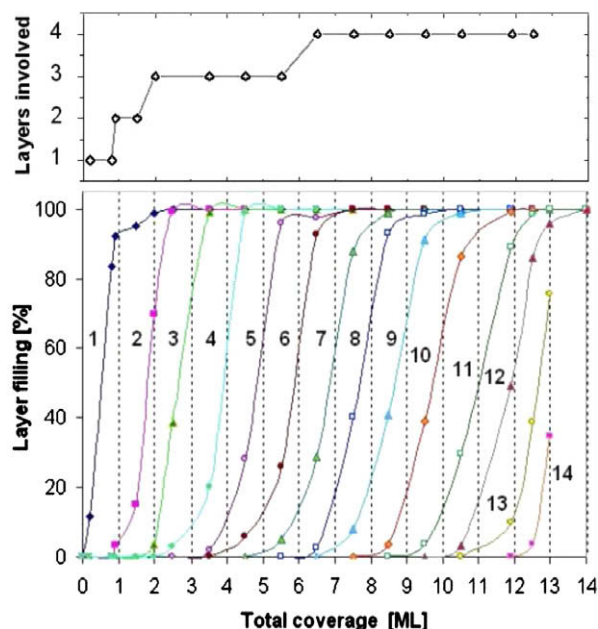


Fig. 7. This plot indicates the layer filling, in percentage, as a function of total Ni mass expressed in ML. The solid lines connects the points associated to a single layer as it is observed for different coverages. Above 2 ML, the growth mode changes from layer-by-layer to multilayer. The insert at the top, indicates the total number of layers present in the corresponding STM image as a function of coverage.

served in Ni homoepitaxy on Ni(100). In this case, because of the absence of strain in the interface plane, the growth is dominated by homogeneous nucleation of monolayer height rectangular islands, which reflects the substrate square symmetry. For Ni/Ni(100), step edges that run along [011] direction together with close-packed (111) facets form the most stable configuration.

It is important to point out that in the Ni/Pd(100), the thickness at which the rectangular islands start to appear is also the onset for multilayer growth. This can be explained by a possible modification of the diffusion energy barriers at a certain critical thickness, as reported in other thin film systems [14,24,27–29]. When the kink site diffusion increases, starting at a certain coverage, the islands tend to show a rectangular shape with edges along the [011] directions, in the case of substrates with square symmetry [24]. On the other hand, an additional Ehrlich–Schwoebel barrier

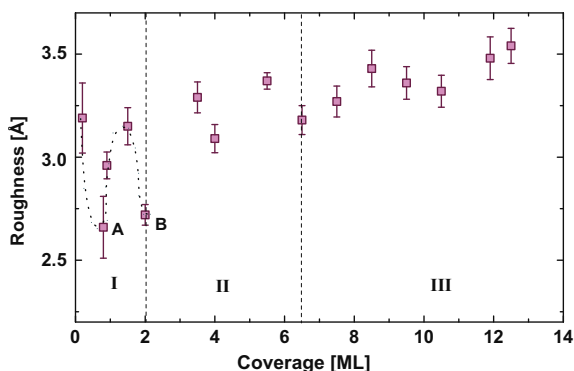


Fig. 8. RMS surface roughness, obtained from STM images, as a function of coverage for Ni/Pd(100). The vertical dotted lines are meant to separate different growth modes. Up to 2 ML the characteristic growth is layer-by-layer. Index A and B correspond to roughness minimum value, which are in coincidence with the completion of the first and the second layer. Region II corresponds to multilayer growth with 3 layers exposed on the surface. In region III, 4 layers are involved in growth. The dotted line is to guide the eye.

has been reported in other heteroepitaxial systems [14,27–29] above a critical thickness. This barrier, modified by the film strain, can influence directly the transition from 2D to 3D growth, a process which seems to be in agreement with our experimental results.

From 6.5 ML to 10.5 ML a new interlayer distance, close to 1 Å, occurs simultaneously with the appearance of filament-like structures. This behavior is presumably connected with the strain relief mechanism associated to fct films.

Similar structures have been reported in other metallic thin film systems, starting at a critical thickness [30,31]. They do have in common with ours, a large *tensile* strain value (14% in the case of Fe on Au(100) and 7.8% for Cu on Pd(100)). However, in spite of the morphological resemblance of the structure, the proposed structural models, based on bcc(110) growth on a bcc(100) substrate and misfits dislocations, cannot be adjusted to the Ni/Pd(100) system. Most likely the 1 Å height has its origin on Ni atoms laterally displaced away from their expected hollow site positions.

Interlayer distances determined from step height variations in STM, can be attributed to a physical change in height, only if the local density of states on the terraces in both sides of the steps are equivalent, from the point of view of the tunneling process. From our results this is not the case for the surface formed at 6.5 ML Ni/Pd (see profile Fig. 3b), since the structure of the top Ni terrace is indeed different from the layer below. A similar situation occurs for sub-monolayer coverages. These structural differences can modify the top layer electronic structure, which in turn determines the apparent height between two terraces. Nevertheless, in the case of Ni/Pd, for 7.5 ML and higher coverages, the new layers are all 1 Å apart and growing on top of a “similar” underlying structure. The lack of a smooth coverage dependence of the interlayer distance, seems to indicate a negligible electronic effect on the apparent atomic step height, as is expected for metallic surfaces.

Multilayer growth at large coverages involves simultaneously four layers, a value which is maintained from this point on, up to the largest coverage we measured. Finally above 10.5 ML the films recover their fcc lattice parameters (reaching an average value 1.74 Å for the interlayer distance). The surface exhibits now

(Fig. 4c) a net-like appearance that dominates the complete landscape. Similar structures have also been observed in other fcc(100) heteroepitaxial systems [31].

5. Summary

We have described the RT growth of Ni/Pd(100). This surface exhibits a transition from pseudomorphical fct to fcc growth over a range of 4 ML. In this transition region a new apparent surface interlayer distance is established and this happens in conjunction with the appearance of narrow filaments over the surface. The presence of these filaments at higher coverages seems to determine the surface structure and the formation of a superstructure rectangular network, once the fcc growth is recovered. In future work we expect to correlate the evolution of the film structure with the magnetic properties of thin layers.

Acknowledgements

This work has been supported by CONICYT-Programa Bicentenario de Ciencia y Tecnología, Chile (CENAVA, Grant# ACT-027) and the L’Oreal-UNESCO Women on Science program.

References

- [1] J. Shen, J. Kirschner, Surf. Sci. 500 (2002) 300.
- [2] J. Giergel, J. Shen, J. Woltersdorf, A. Kirilyuk, J. Kirschner, Phys. Rev. B 52 (1995) 8528.
- [3] K. Kalki, D.D. Chambliss, K.E. Johnson, R.E. Johnson, R.J. Wilson, S. Chiang, Phys. Rev. B 48 (1993) 18344.
- [4] A. Biedermann, M. Schmid, P. Varga, Phys. Rev. Lett. 86 (2001) 464.
- [5] A. Biedermann, R. Tseliebniq, M. Schmid, P. Varga, Phys. Rev. Lett. 87 (2001) 086103.
- [6] A. Biedermann, R. Tseliebniq, M. Schmid, P. Varga, Appl. Phys. A 78 (2004) 807.
- [7] A. Kirilyuk, J. Giergel, J. Shen, M. Straub, J. Kirschner, Phys. Rev. B 54 (1996) 1050.
- [8] S. Müller, P. Beyer, C. Reischl, K. Heinz, B. Feldmann, H. Zillgen, M. Wuttig, Phys. Rev. Lett. 74 (1995) 765.
- [9] P. Xhonneux, E. Courtens, Phys. Rev. B 46 (1992) 556.
- [10] D. Qian, X.F. Jin, J. Barthel, M. Klaua, J. Kirschner, Phys. Rev. B 66 (2002) 172406.
- [11] G.A. Rizzi, M. Petukhov, M. Sambì, G. Granozzi, Surf. Sci. 522 (2003) 1.
- [12] M. Petukhov, G.A. Rizzi, M. Sambì, G. Granozzi, Appl. Surf. Sci. 212 (2003) 264.
- [13] G.A. Rizzi, A. Cossaro, M. Petukhov, F. Sedona, G. Granozzi, F. Bruno, D. Cvetko, A. Morgante, L. Floreano, Phys. Rev. B 70 (2004) 45412.
- [14] J. Shen, J. Giergel, J. Kirschner, Phys. Rev. B 52 (1995) 8454.
- [15] S. Heinrichs, J. Rottler, P. Maass, Phys. Rev. B 62 (2000) 8338.
- [16] J. Krug, P. Politi, T. Michely, Phys. Rev. B 61 (2000) 14037.
- [17] J. Tersoff, A.W. Denier van der Gon, R.M. Tromp, Phys. Rev. Lett. 72 (1994) 266.
- [18] J. Rottler, P. Maass, Phys. Rev. Lett. 83 (1999) 3490.
- [19] C. Parra, P. Häberle, M.D. Martins, W.A.A. Macedo, Microelectr. J. 39 (2008) 1229.
- [20] P.M. Marcus, F. Jona, Surf. Rev. Lett. 1 (1994) 15.
- [21] I. Horcas, Rev. Sci. Instrum. 78 (2007) 013705.
- [22] Elmar Hahn, Elisabeth Kampshoff, Nicolas Wlchli, Klaus Kern, Phys. Rev. Lett. 74 (1995) 1803.
- [23] P. Blandin, C. Massobrio, P. Ballone, Phys. Rev. Lett. 72 (1994) 3072.
- [24] Y. Saito, Phys. Soc. Jpn. 72 (2003) 2008.
- [25] Jianxin Zhong, Tianjiao Zhang, Zhenyu Zhang, Max G. Lagally, Phys. Rev. B 63 (2001) 113403.
- [26] E. Somfai, L.M. Sander, Condens. Matter Mater. Sci. arXiv:cond-mat/9909328v1.
- [27] J. Vrijmoeth, H.A. van der Vegt, J.A. Meyer, E. Vlieg, R.J. Behm, Phys. Rev. Lett. 72 (1994) 3843.
- [28] J.A. Meyer, J. Vrijmoeth, H.A. van der Vegt, E. Vlieg, R.J. Behm, Phys. Rev. B 51 (1995) 14790.
- [29] Ki-Ha Hong, Jong-Kyu Yoon, Pil-Ryung Cha, Appl. Surf. Sci. 253 (2006) 2776.
- [30] V. Blum, Ch. Rath, S. Müller, L. Hammer, K. Heinz, J.M. García, J.E. Ortega, Phys. Rev. B 59 (1999) 15966.
- [31] Y. Lu, M. Przybłski, O. Trushin, W.H. Wang, J. Barthel, E. Granato, S.C. Ying, T. Ala-Nissila, Phys. Rev. Lett. 94 (2005) 146105.